The Journal of Immunology

RESEARCH ARTICLE | JULY 15 2022

CD11b^{high} B Cells Increase after Stroke and Regulate Microglia

Janelle M. Korf; ... et. al

J Immunol (2022) 209 (2): 288–300.
https://doi.org/10.4049/jimmunol.2100884

CD11b^{high} B Cells Increase after Stroke and Regulate Microglia

Janelle M. Korf,*,†,[1] Pedram Honarpisheh,*,†,[1] Eric C. Mohan,* Anik Banerjee,† Maria P. Blasco-Conesa,* Parisa Honarpisheh,* Gary U. Guzman,* Romeesa Khan,* Bhanu P. Ganesh,* Amy L. Hazen,‡ Juneyoung Lee,* Aditya Kumar,* Louise D. McCullough,* and Anjali Chauhan*

Recent studies have highlighted the deleterious contributions of B cells to post-stroke recovery and cognitive decline. Different B cell subsets have been proposed on the basis of expression levels of transcription factors (e.g., T-bet) as well as specific surface proteins. CD11b (α-chain of integrin) is expressed by several immune cell types and is involved in regulation of cell motility, phagocytosis, and other essential functions of host immunity. Although B cells express CD11b, the CD11b^{high} subset of B cells has not been well characterized, especially in immune dysregulation seen with aging and after stroke. Here, we investigate the role of CD11b^{high} B cells in immune responses after stroke in young and aged mice. We evaluated the ability of CD11b^{high} B cells to influence pro- and anti-inflammatory phenotypes of young and aged microglia (MG). We hypothesized that CD11b^{high} B cells accumulate in the brain and contribute to neuroinflammation in aging and after stroke. We found that CD11b^{high} B cells are a heterogeneous subpopulation of B cells predominantly present in naive aged mice. Their frequency increases in the brain after stroke in young and aged mice. Importantly, CD11b^{high} B cells regulate MG phenotype and increase MG phagocytosis in both ex vivo and in vivo settings, likely by production of regulatory cytokines (e.g., TNF-α). As both APCs and adaptive immune cells with long-term memory function, B cells are uniquely positioned to regulate acute and chronic phases of the post-stroke immune response, and their influence is subset specific. ***The Journal of Immunology*****, 2022, 209: 288–300.**

Age-related changes in the immune system are a determining factor in clinical outcomes of neurologic diseases, including stroke (1, 2). Work from our laboratory and others has shown that immune cell populations from aged animals can be significantly different in relative frequency and tissue distribution compared with those from young animals, even in the absence of tissue injury (2–4). After ischemic stroke, aged mice have a smaller infarction size than young mice; however, aged mice demonstrate worse neurologic outcomes (5–7). Peripheral immune cells are critical to stroke recovery, and aged peripheral immune cells contribute to greater neurologic deficits and dystrophic changes in microglia (MG) (2, 8). Microglia mount a proinflammatory response to infarction, perform phagocytosis, and present Ags for the gradual recruitment of adaptive immune cells (9). After injury, the dural meninges and eventually the brain parenchyma are infiltrated by peripheral leukocytes, further amplifying the immune response (10). Damage to the blood–brain barrier results in loss of integrity, allowing a greater influx of peripheral leukocytes into the brain parenchyma (11, 12). Importantly, both brain-resident MG and long-lived peripheral B cells undergo significant age-related changes (13–16).

Aged MG contribute to detrimental immune responses, chronic inflammation, and poorer outcomes after brain injury (2, 17). Aged MG have a transcriptomic profile indicative of a chronic proinflammatory state, characterized by increased proinflammatory cytokine production (e.g., TNF-α, IL-1β, and IL-6), genes associated with host defense, and cell adhesion (18–21). MG are key producers of and are regulated by TNF-α after injury (22). TNF-α participates in injury-mediated MG and astrocyte activation and MG phagocytosis (22–25). TNF-α can be secreted from a variety of cell types, including long-lived adaptive immune cells such as B cells (26).

B cells have multiple subtypes and diverse roles after stroke (27). For example, IL-10 secretion by regulatory B cells reduces infarct

*Department of Neurology, University of Texas McGovern Medical School, Houston, TX; †University of Texas MD Anderson Cancer Center, UTHealth Graduate School of Biomedical Sciences, Houston, TX; ‡University of Texas McGovern Medical School, Brown Foundation Institute of Molecular Medicine for the Prevention of Human Diseases, Houston, TX

[1]J.M.K. and Pedram Honarpisheh contributed equally to this study.

ORCIDs: 0000-0003-0246-6894 (J.M.K.); 0000-0002-9126-6271 (Pedram Honarpisheh); 0000-0003-4950-9716 (E.C.M.); 0000-0002-8902-7976 (Parisa Honarpisheh); 0000-0001-8002-9994 (G.U.G.); 0000-0002-4129-1612 (R.K.); 0000-0002-8050-1686 (L.D.M.).

Received for publication September 9, 2021. Accepted for publication April 22, 2022.

This work was supported by the Center for Clinical and Translational Sciences TL1 Training Program, National Institutes of Health (NIH) Grant TL1 TR003169 (to Pedram Honarpisheh), NIH/National Institute of Neurological Disorders and Stroke (NINDS) Grant 1F31NS118984-01 (to Pedram Honarpisheh), NIH/National Institute on Aging (NIA), and NINDS grants 5-R01-NS103592-02 (Detrimental Effects of Age Related Dysbiosis to L.D.M.), NIH/NIA 1-R01-AG070934-01 (Link between Early Gut Dysfunction and Amyloid Beta Aggregation in Alzheimer's Disease Related Dementia to B.P.G.), NINDS Exploratory Neuroscience Research Grant 1 R21 NS114836-01A1 (Role of CD13 in Ischemic Stroke to A.C.), and NIH/NINDS 5-R01-NS094543-04 (Reversing Age Related Inflammation to L.D.M.).

J.M.K. and Pedram Honarpisheh contributed equally to the study and were involved in the study design, completion of all experiments, data analysis and interpretation, and manuscript preparation. E.C.M., A.B., Parisa Honarpisheh, G.U.G., R.K., M.P.B.-C., and J.L. were involved in performing flow cytometry experiments and sample collection. A.C. performed the middle cerebral artery occlusion surgeries. B.P.G., A.L.H., J.L., A.K., L.D.M., and A.C. were involved in the data interpretation and manuscript editing. A.C. and L.D.M. were involved in study design and manuscript preparation.

Address correspondence and reprint requests to Anjali Chauhan, University of Texas McGovern Medical School, 6431 Fannin Street, Houston, TX 77030. E-mail address: anjali.chauhan@uth.tmc.edu

The online version of this article contains supplemental material.

Abbreviations used in this article: AD, Alzheimer's disease; EAE, experimental autoimmune encephalomyelitis; MFI, median fluorescence intensity; MG, microglia; MCAO, middle cerebral artery occlusion; P2RY12, purinergic receptor P2Y12; tSNE, *t*-distributed stochastic neighbor embedding; Tmem119, transmembrane protein 119.

size and inflammation in mice (27, 28), and B cell production of IgG facilitates opsonization of myelin debris for clearance by microvascular endothelial cells and macrophage recruitment (29). Conversely, detrimental responses also arise from B cells. After stroke, brain Ags are exposed to the periphery, and APCs from the brain migrate to the cervical lymph nodes, leading to the amplification of harmful autoreactive lymphocytes and chronic inflammation (30).

Most myeloid cells, as well as B cells, express CD11b for regulation of cell motility and phagocytosis (31, 32). A distinct subset of B cells have been found to accumulate in aged mice and have been studied in the context of autoimmune diseases (33–35). However, less is known regarding the role of aged B cell subsets after stroke (36, 37). Different aged B cells subsets have been proposed on the basis of expression levels of transcription factors (e.g., T-bet) as well as surface proteins, including CD11b (38–41). CD11b^{high} B cells are often excluded in common approaches in flow cytometric brain immunophenotyping (42–46). Our data show that the relative frequency of CD11b^{high} B cells significantly increases with aging and after stroke in both young and aged mice. Sorting peripheral B cells into two subsets of CD11b^{low} and CD11b^{high} revealed significant differences in their surface phenotype, inflammatory cytokine production, and phagocytic activity (Fig. 1). We hypothesized that CD11b^{high} B cells increase in the brain and contribute to neuroinflammation in aging and after stroke by regulating MG activation and phagocytosis. We demonstrated that CD11b^{high} B cells can produce higher levels of TNF-α than their CD11b^{low} counterparts, which can activate MG phagocytosis. Taken together, our results emphasize the nuances of immunophenotyping of brain CD11b^{high} and CD11b^{low} B cell subsets in age-related neuroinflammation.

Materials and Methods

Mice

Young (2–4 months) and aged (18–22 months) C57BL/6J male wild-type mice from the NIA were used in this study. PepBoy mice (from The Jackson Laboratory) are a congenic strain that carries the differential Ptprc pan-leukocyte marker commonly known as CD45.1. C57BL/6 inbred mice express the Ptprc (CD45.2) allele. CD45 is a common B Ag expressed in all leukocytes. It has two different alleles, CD45.1 and CD45. 2, which are functionally identical. This allows the differentiation of transferred B cells from (CD45.2) mice (donor) to recipient PepBoy (CD45.1) mice because of the different CD45 alleles (CD45.1 versus CD45.2). All animals were group housed in Tecniplast individually ventilated cage racks, fed a commercially available irradiated, balanced mouse diet (no. 5058, LabDiet, St Louis, MO), and provided corncob bedding. Rooms were maintained at 21–24°C under a 12-h/12-h light/dark cycle. All animals were maintained in specific pathogen-free conditions (see Supplemental Table I for a list of monitored pathogens). Animal procedures were performed at an Association for Assessment and Accreditation of Laboratory Animal Care–accredited facility and were approved by the Animal Welfare Committee at the University of Texas Health Science Center in Houston, TX.

Middle cerebral artery occlusion (MCAO)

Transient focal ischemia was induced under isoflurane anesthesia in young or aged mice for 60 min by occlusion of the right middle cerebral artery (47). Body temperature was maintained at 37.0 ± 1.0°C throughout the surgery by an automated temperature control feedback system (TC1000, mouse, CWE). A midline ventral neck incision was made, and unilateral MCAO was performed by inserting a Doccol monofilament (Doccol Corp., Redlands, CA) into the right internal carotid artery. One hour after ischemia, animals were anesthetized again, and reperfusion was established by withdrawal of the monofilament. Animals were then placed in a recovery cage and were euthanized 72 h after reperfusion. Sham control animals were subjected to the same procedure, except the suture was not introduced into the middle cerebral artery. Animals were randomly assigned into the stroke and sham surgery groups and singly housed in their recovery cages for the first 2 h after surgery. Sham and stroke mice were then housed together in their home cages to minimize detrimental effects of social isolation (48). All mice were selected for sham or stroke surgery in a randomized manner, and all analyses were performed blinded to surgical conditions. Animals that died of hemorrhagic transformation or had a neurological deficit score >3 included 13 aged mice (out of 35) and 6 young mice (out of 23). A representative Kaplan-Meier curve is included in Fig. 2D.

Flow cytometry

A previously published brain single-cell suspension protocol was used (2, 49). In brief, mice were euthanized by i.p. avertin injection. Blood was drawn by cardiac puncture with heparinized needles. RBC lysis was achieved by two consecutive 10-min incubations with Tris–ammonium chloride (STEMCELL Technologies). Mice were transcardially perfused with 20 ml cold, sterile PBS before aseptic removal of brain tissues. Brain tissue was placed in complete RPMI 1640 medium (Lonza), then mechanically and enzymatically digested in collagenase/dispase (1 mg/ml; Roche Diagnostics) and DNase (10 mg/ml; Roche Diagnostics) for 45 min at 37°C with gentle shaking (80 rpm). The cell suspension was filtered through a 70-μm cell strainer. Leukocytes were harvested from the interphase of a 70–30% Percoll gradient for the brain tissue after a 20-min centrifugation at room temperature with no brakes. Cells were washed and blocked with Fc receptor block (BioLegend, lot B298973) before staining with the following preconjugated fluorophores: CD45.2-eF450 (eBioscience, catalog no. 48-0451-82), CD45.1-FITC (eBioscience, catalog no. 11045385), CD11b-allophycocyanin (BioLegend, catalog no. 101212), CD19-FITC (BioLegend, catalog no. 101506), Ly6C-PerCP-cyanine 5.5 (Cy5.5) (BioLegend, catalog no. 128011), transmembrane protein 119 (Tmem119)-PE-Cy7 (eBioscience, catalog no. 25-6119-82), purinergic receptor P2Y12 (P2RY12)-PE (BioLegend, catalog no. 848003), MHC class II (MHC-II)-allophycocyanin-Fire750 (BioLegend, catalog no. 107652), IgM-PE-Cy7 (BioLegend, catalog no. 406514), IgD-PE (BioLegend catalog no. 405706), CD268-FITC (Thermo Fisher Scientific catalog no. 11-5943-82), CD27-PerCP-Cy5.5 (BioLegend, catalog no. 124214), CD80-FITC, CD138-allophycocyanin (BioLegend, catalog no. 142506), CD73-PE-Cy7 (BioLegend, catalog no. 127224), T-bet-PE (BioLegend, catalog no. 644810), TNF-α-allophycocyanin (BioLegend catalog no. 506308), and Zombie Aqua (BioLegend, catalog no. 423102). Cell stimulation for cytokine staining was done using Cell Activation Cocktail (with brefeldin A) (BioLegend, catalog no.423304). Cell isolation, Percoll gradient, and immunostaining steps were carried out at once for both control animals and injury models to minimize experimental variability; that is, all sham and stroke samples were processed together, and all naive young and aged samples were processed together. Data were acquired on a Cytoflex-S device (Beckman Coulter) or BD FACSMelody (BD Biosciences) and analyzed using FlowJo (BD Biosciences). No less than 300,000 events were recorded for each sample. Tissue-matched and injury-matched fluorescence-minus-one and unstained controls were used to aid in positive gating strategy (Supplemental Fig. 1A). *t*-Distributed stochastic neighbor embedding (tSNE) plots were generated in FlowJo using the DownSample plug-in (3000 cells per sample for each study group) followed by the tSNE algorithm on all compensated parameters (except viability) at 1000 iterations, perplexity of 30, learning rate of 5040, and Barnes-Hut gradient algorithm.

Cell sorting

Single-cell suspension and surface staining were performed as described above. After viability and single-cell selections, MG gated as live Tmem119^{+} (verified to be CD45^{int}CD11b^{+}) were sorted under an aseptic hood from the single-cell suspension prepared from naive aged male brains (full brains, $n = 8$), stroke aged male brains (full brains, $n = 4$), and naive young male brains (full brains, $n = 4$) using BD FACSMelody.

After viability and single-cell selections, B cells, gated as live CD45^{+}CD19^{+}, were sorted under the hood from the single-cell suspension prepared from naive or stroke aged male spleens (spleen, $n = 14$) using BD FACSMelody. Fluorescence-minus-one and unstained controls were used to aid in the positive gating strategy to delineate CD11b^{high} from CD11b^{low} and CD11b^{neg} B cells. Sorting was performed from the tube directly into the 96-well plate used for coincubation experiments to preserve cell counts and into FACS tubes for adoptive transfer experiments. Cell counts were conducted in ratios similar to what was analyzed from our post-stroke data (i.e., 1:1000 MG to CD11b^{high} B cells and 1:100 MG to CD11b^{low} B cells), to maintain the physiologic relevance of our ex vivo experimental conditions. Each sorted sample was then divided (by volume) into control or coincubated cohorts with each B cell subset for 4 h under a sterile cell culture environment. Cells were then washed with PBS, stained for surface markers and viability after the 4-h coincubation, and then analyzed by flow cytometry.

Adoptive B cell transfer

Donor mice were 18–20 mo old so that they would a have sufficient number of cells to collect for transfer. Naive or stroke mice were euthanized, and immune cells collected postmortem. Using the BD FACSMelody cell sorting

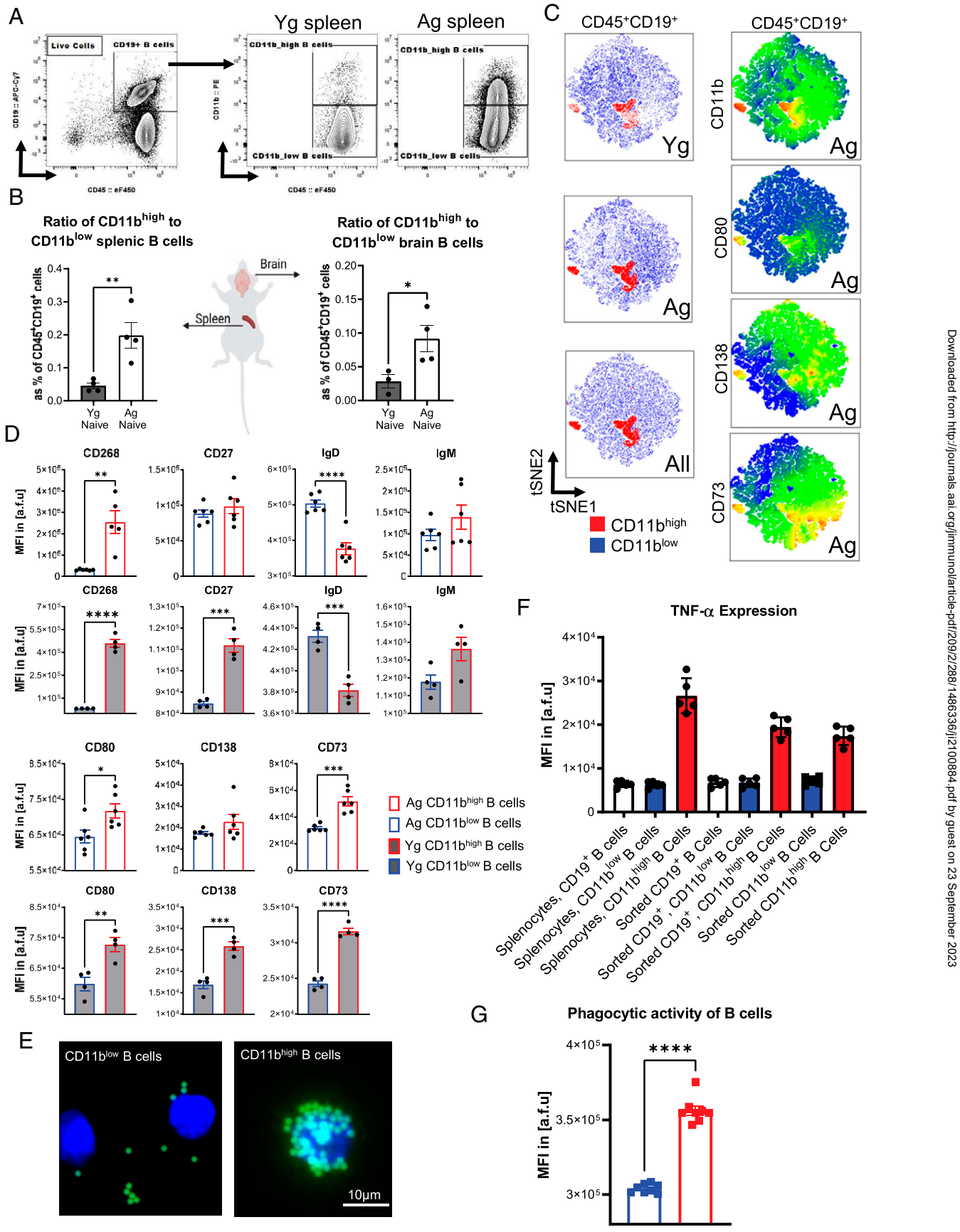

FIGURE 1. CD11b^{high} B cells increase with aging and have a distinct surface phenotype, increased TNF-α production, and increased phagocytosis. (**A**) Representative gating strategy from cells/singlets/live/CD45$^+$/CD19$^+$ B cells in naive young (Yg) and aged (Ag) mice. (**B**) The ratio of CD11b^{high} to CD11b^{low} B cells isolated from spleen and brain in Yg ($n = 4$) and Ag ($n = 5$) naive animals (spleen, $p = 0.0089$; brain, $p = 0.0466$; unpaired t test). Absolute counts listed in Table I. Results were reproduced in two independent experiments. (**C**) The first column represents a *(Figure legend continues)*

Table I. Absolute counts of naive brain and spleen B cell populations for Fig. 1B

Tissue	Naive Group	$CD11b^{high}$ B Cells (Average ± SD)	$CD11b^{low}$ B Cells (Average ± SD)	Sample Size
Spleen	Aged	28,485.6 ± 5,895.95	102,279.80 ± 20,288.60	5
	Young	23,032.25 ± 3,647.26	95,702.75 ± 11,175.64	4
Brain	Aged	96.40 ± 64.92	595.40 ± 441.76	5
	Young	4.75 ± 5.19	166.75 ± 62.78	4

system, a pure cell population of ~50,000 CD11b-expressing B lymphocytes were collected for adoptive transfer into a single recipient mouse. One donor mouse for every one recipient mouse was required to have an adequate number of cells. The number of cells (50,000) was determined by the physiologic amount we detected in aged and stroke mice. Cells were resuspended in 37°C PBS and retro-orbitally injected into the anesthetized recipient using a BD insulin syringe with the BD Ultra-Fine needle (12.7 mm × 30-gauge, 3/10 ml/cc).

Ex vivo coincubation experiments

Collection and isolation of brain monocytes was performed by optimized enzymatic digestion followed by a Percoll gradient protocol (2, 49). Brain tissue was harvested after cardiac perfusion with PBS to eliminate blood from the brain tissue. There is a possibility that PBS-perfused samples contain some blood-sourced immune cells before ex vivo coincubation. Thus, we performed digestion and Percoll gradient–based separation of MG, at which point each individual single-cell suspension of CNS mononuclear cells was divided (by equal volumes) into a two or three coincubation conditions with different B cell subsets (Fig. 1). Coincubated cells were kept in a sterile cell culture environment at 37°C for 4 h and 24 h.

Phagocytosis assay

A quantity of 0.5 μm Fluoresbrite 641–conjugated carboxylate microspheres (1 μl stock solution/200 μl in a 96-well plate) (50) were added to sorted MG or to CNS mononuclear cells enriched in MG (from a brain that is postdigestion and post–Percoll gradient protocol) and incubated for 4 or 24 h. Cell mixtures were incubated with beads for 30 min at 37°C. Afterward, cells were washed twice with PBS and then stained for flow cytometry following the previous protocol.

Microscopy

Images were obtained on a Keyence BZ-X810 all-in-one fluorescence microscope at 40× and 60× magnification. Images were processed for brightness and contrast correction, cropping, and addition of scale bars with Keyence BZ-X800 Analyzer 1.1.1.8 software.

Statistical analysis

Statistical analysis for flow cytometric data was performed using an unpaired *t* test, one-way ANOVA, and paired one-way ANOVA with post hoc analysis, with all related *p* values adjusted by Dunnett's or Tukey's methods for multiple comparisons (specified in the figure legends). Statistical significance was considered at $p < 0.05$, and $*p < 0.05$, $**p < 0.01$, $***p < 0.001$, and $****p < 0.0001$ convention was used in the presented figures. All statistical analyses were performed with GraphPad Prism 7.

Results

$CD11b^{high}$ B cells increase with aging and have a distinct surface phenotype, increased TNF-α production, and increased phagocytosis

First, we provided a representative gating strategy from cells/singlets/live/$CD45^+/CD19^+$ B cells in naive aged and young mice to demonstrate the significant increase in relative frequency of $CD11b^{high}$ B cells in aged mice (Fig. 1A and Supplemental Fig. 1A). The increased ratio of $CD11b^{high}$ to $CD11b^{low}$ B cells with aging was independent of tissue origin (spleen or brain) (Fig. 1B and Table I). We then performed multidimensional flow cytometric phenotyping of $CD11b^{high}$ B cells. We asked if $CD11b^{high}$ B cells were predominated by mature B cells, memory B cells, or class-switched B cells using expression of CD73, CD138, and CD80, respectively. Results are depicted in a tSNE map superimposed with heatmaps for each surface marker (Fig. 1C). Individual gating revealed an increase in CD80 and CD73 median fluorescence intensities (MFIs) in $CD45^+CD19^+CD11b^{high}$ compared with $CD45^+CD19^+CD11b^{low}$ splenic B cells of young and aged naive mice, with plasma cell marker CD138 MFI also significantly increased in $CD45^+CD19^+CD11b^{high}$ of young naive mice (Fig. 1D). A significant increase in CD27 (young, $p = 0.0002$) supports a memory B cell phenotype within the $CD11b^{high}$ B cell population. To understand the functional role of $CD11b^{high}$ B cells, we examined surface phenotype markers CD268, IgD, and IgM expression (Fig. 1D) on $CD45^+CD19^+CD11b^{high}$ compared with $CD45^+CD19^+CD11b^{low}$ B cells isolated from splenocytes of young ($n = 4$) and aged ($n = 6$) naive mice. $CD45^+CD19^+CD11b^{high}$ B cells showed a significant increase in CD268 (aged, $p = 0.0011$ and young $p < 0.0001$), a significant decrease in IgD (aged, $p < 0.0001$; young, $p = 0.0008$), and no significant changes in IgM in young or aged B cells compared with aged-matched $CD45^+CD19^+CD11b^{low}$ (Fig. 1D). The relative frequency of these populations varied (Supplemental Fig. 2A, 2B). Together, these observations indicated that the $CD11b^{high}$ B cells are a mixed population of B cell subsets. We also examined $CD11b^{high}$ B cells from the spleen, blood, and skull bone marrow of young and aged stroke mice, which showed a distinct surface phenotype from $CD11b^{low}$ B cells (Supplemental Fig. 2C–2E). These observations suggest that $CD11b^{high}$ B cells increase in the periphery and in the brain with aging in the absence

tSNE plot of $CD45^+/CD19^+$ cells demonstrating the $CD11b^{high}$ (red) and $CD11b^{low}$ (blue) subpopulations of B cells in Yg, Ag, and combined populations as well as the increase in $CD11b^{high}$ B cells with aging. The second column demonstrates a heatmap of the coexpression of B cell–associated surface markers (CD11b, CD80, CD138, and CD73) in Ag B cells. (**D**) Surface phenotype in MFI of $CD45^+/CD19^+/CD11b^{high}$ compared with $CD45^+/CD19^+/CD11b^{low}$ B cells isolated from splenocytes of naive Ag ($n = 6$) and Yg ($n = 4$) mice. Data reproduced in two independent experiments. The top two rows show a significant increase in CD268 in Ag ($p = 0.0011$) and Yg ($p < 0.0001$) cells, no significant change in CD27 in Ag ($p = 0.3944$) with an increase in Yg ($p = 0.0002$) cells, a decrease in IgD (Ag, $p < 0.0001$; Yg, $p = 0.0008$) cells, and no significant changes in IgM in Ag ($p = 0.2075$) and Yg ($p = 0.00529$) cells. The bottom two rows show a significant increase in CD80 in Ag ($p = 0.0208$) and Yg ($p = 0.0064$) cells, an increase in CD138 in Yg ($p = 0.0006$) with no change in Ag ($p = 0.1786$) cells, and an increase in CD73 in Ag ($p = 0.0002$) and Yg ($p < 0.0001$) cells. (**E**) Phagocytosis of 1 μm FITC fluorescent beads by sorted cells/singlets/live/$CD45^+/CD19^+$ $CD11b^{high}$ and $CD11b^{low}$ B cells from splenocytes isolated from Ag naive animals ($n = 8$). Representative images of 1 μm FITC fluorescent beads with $CD11b^{low}$ (left) $CD11b^{high}$ (right) B cells stained with DAPI. (**F**) FACS detection of TNF-α production in $CD11b^{high}$ and $CD11b^{low}$ B cells from sorted $CD45^+/CD19^+/CD11b^{high}$, sorted $CD45^+/CD19^+/CD11b^{low}$, sorted $CD45^+/CD19^+$, and splenocytes isolated from Ag naive animals ($n = 5$). (**G**) FACS analysis of phagocytosis of fluorescent beads by splenocytes, sorted cells/singlets/live/$CD45^+/CD19^+$ B cells, and sorted cells/singlets/live/$CD45^+/CD19^+$ $CD11b^{high}$ and sorted cells/singlets/live/$CD45^+/CD19^+$ $CD11b^{low}$ B cells from splenocytes isolated from Ag naive animals ($n = 5$). B–D, F, and G results reproduced in two independent experiments. Unpaired *t* test. Mean ± SEM. $*p < 0.05$, $**p < 0.01$, $***p < 0.001$, $****p < 0.0001$.

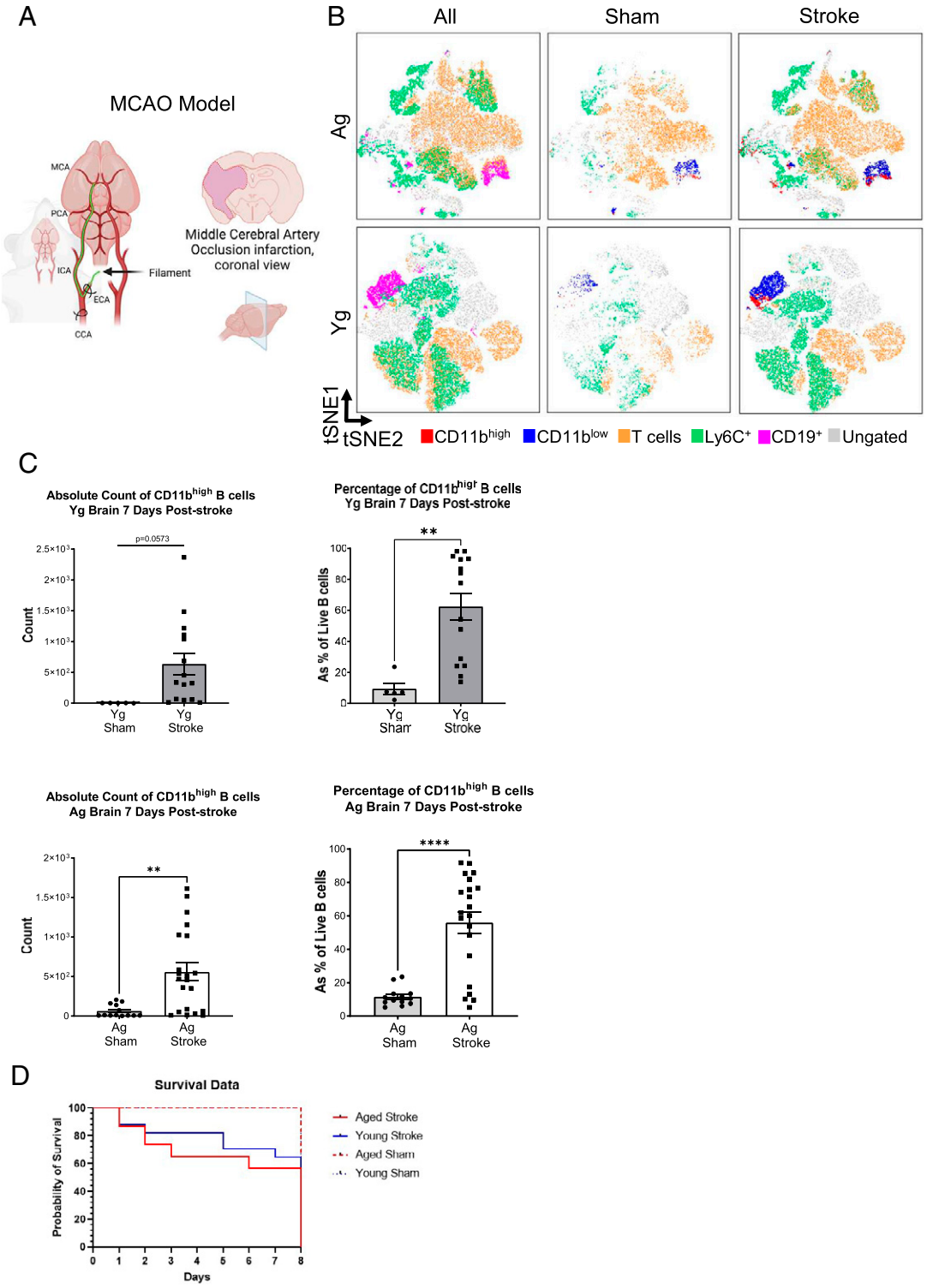

FIGURE 2. CD11b^{high} B cells are increased to both young and aged brains as early as post–MCAO day 7. (**A**) Schematic of the MCAO model used for inducing neurologic injury in mice. (**B**) tSNE plots of live CD45^{high} cells (non-MG immune cells) from sham and stroke homogenized brain from young (Yg) and aged (Ag) mice, demonstrating CD19^{+} B cells (pink), CD11b^{high} B cells (red), CD11b^{low} B cells (blue), CD3^{+} T cells (orange), Ly6C^{+} monocytes (green), and ungated populations (gray), indicating the increase in CD11b^{high} B cells after stroke when compared with sham in both Yg and Ag MCAO mice. (**C**) Quantification of CD11b^{high} and CD11b^{low} B cells isolated from brain, comparing the absolute counts and percentages of CD19^{+} cells from sham control animals with the ipsilateral hemisphere in stroke animals. Experiments were conducted in both Yg (n = 5–15) and Ag mice (n = 13–21). Left, The ipsilateral stroke hemisphere in Ag animals demonstrates a significant increase in CD11b^{high} B cells (p = 0.0019), with Yg cells trending upward in number (p = 0.0573). Right, The ipsilateral stroke hemisphere in Ag and Yg animals demonstrates a significant increase in the percentage of CD11b^{high} B cells within the total CD45^{+}/CD19^{+} B cell population ($p < 0.0001$ and p = 0.0027, respectively). (**D**) Representative Kaplan-Meier curve for MCAO mortality in Ag and Yg mice. Results were compiled from six independent experiments. Outlier test robust regression with outlier removal (Q = 1%) was performed on Yg and Ag groups, resulting in the removal of one Yg sham and two Yg stroke samples. Outliers were removed before analysis. Unpaired analysis t test; mean ± SEM. $^{**}p < 0.01$, $^{****}p < 0.0001$.

Table II. Absolute cell counts from right brain hemisphere in Fig. 2

	Group	$CD45^+/CD19^+$ B Cell (Average ± SEM)	$CD11b^{high}$ B Cell (Average ± SEM)	$CD11b^{low}$ B Cell (Average ± SEM)
Aged	MCAO	1111 ± 201.3	557.6 ± 113.2	367.7 ± 101.2
	Sham	830.3 ± 251.1	63.31 ± 21.85	735.9 ± 235.9
Young	MCAO	1321 ± 449.2	635 ± 176.6	595.2 ± 383.3
	sham	63.29 ± 22.03	3 ± 0.55	54 ± 21.59

of any brain injury. Furthermore, $CD11b^{high}$ B cells are a highly activated, heterogeneous subset of B cells with distinct surface phenotype from their $CD11b^{low}$ B cell counterparts.

To verify that B cells can increase their expression of CD11b under proinflammatory conditions, we incubated sorted $CD45^+CD19^+$ B cells with LPS for 48 h. Indeed, our data showed that CD11b expression is

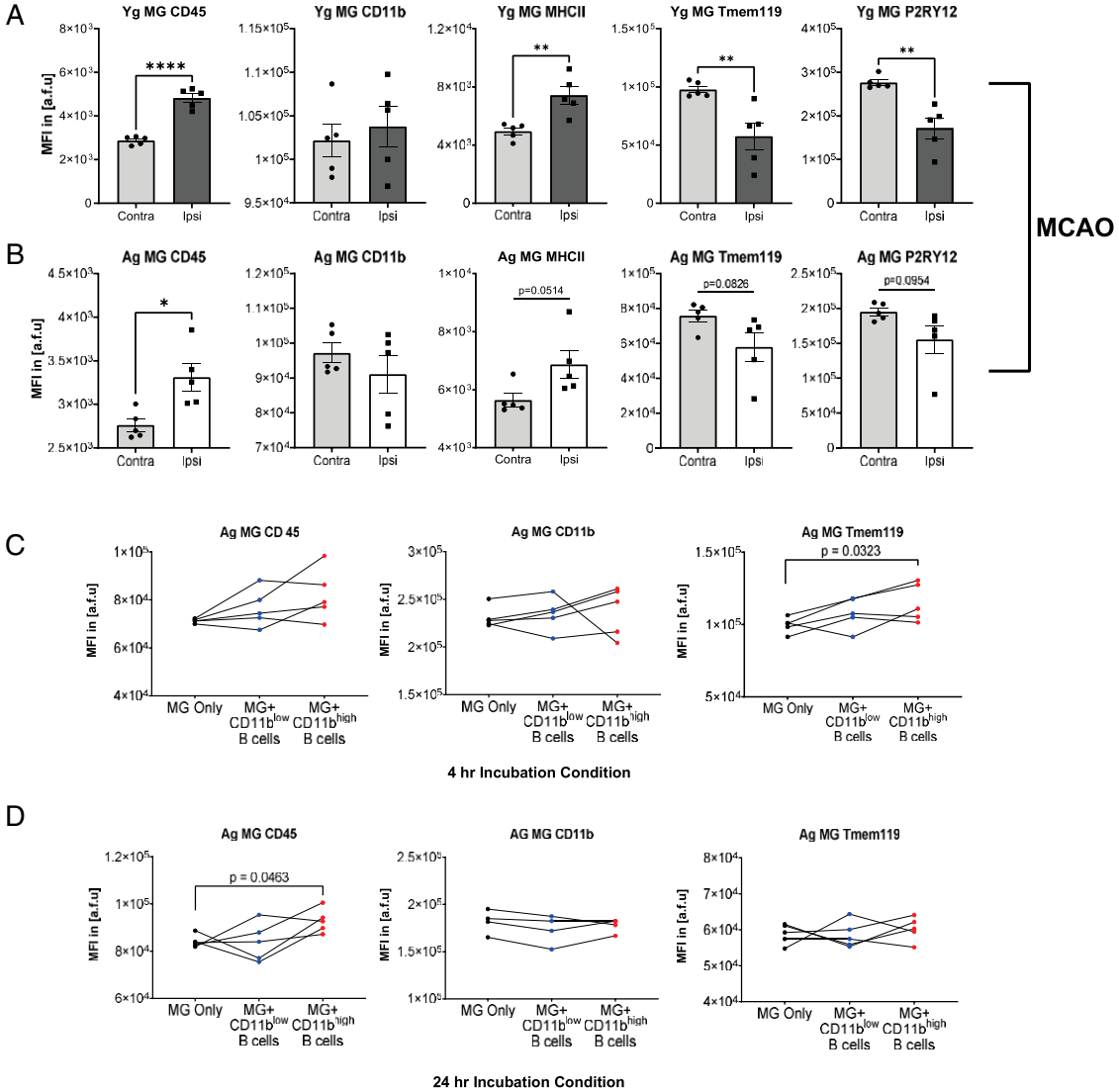

FIGURE 3. Differential MG surface phenotype after stroke and after incubation with sorted $CD11b^{high}$ or $CD11b^{low}$ B cells. (**A**) Surface profile of MG from young (Yg) mice after MCAO comparing contralateral hemisphere and ipsilateral hemispheres. CD45 MFI increased in MG in the ipsilateral hemisphere ($p < 0.0001$), CD11b MFI in MG had no significant change in the ipsilateral hemisphere, MHC-II MFI significantly increased in MG in the ipsilateral hemisphere ($p = 0.0048$), P2RY12 MFI decreased in MG in the ipsilateral hemisphere ($p = 0.0026$), and Tmem119 MFI decreased in MG in the ipsilateral hemisphere ($p = 0.0098$). (**B**) Surface profile of MG from aged (Ag) mice after MCAO comparing contralateral hemisphere and ipsilateral hemispheres. CD45 MFI increased in MG in the ipsilateral hemisphere ($p = 0.0119$), CD11b, MHC-II, Tmem119, and P2RY12 MFI in MG had no significant change in the ipsilateral hemisphere. Ag MG-enriched CNS mononuclear cells respond differently after incubation with $CD11b^{high}$ or $CD11b^{low}$ B cells sorted from Ag splenocytes after 4-h and 24-h incubations. (**C**) Analysis of MG derived from Ag mice and coincubated with B cells sorted from the same respective animal. Post–Percoll gradient brain homogenate was divided across three incubation conditions for paired comparison. MG after a 4-h coincubation with $CD11b^{low}$ B cells, $CD11b^{high}$ B cells, or alone resulted in no significant changes in CD45 or CD11b MFI, and Tmem119 MFI significantly increased ($p = 0.0323$) in $CD11b^{high}$ B cells compared with MG alone. (**D**) Using the same design as (C) with a longer 24-h coincubation with $CD11b^{low}$ B cells, $CD11b^{high}$ B cells, or alone resulted in CD45 MFI significantly increasing ($p = 0.0463$) and no significant changes in CD11b MFI or Tmem119 MFI in $CD11b^{high}$ B cells compared with MG alone. (A) and (B) were reproduced in two independent experiments and analyzed by unpaired one-way ANOVA. (C) and (D) were performed once and analyzed by paired one-way ANOVA with Dunnett's multiple comparisons test. Mean ± SEM. $*p < 0.05$, $**p < 0.01$, $****p < 0.0001$.

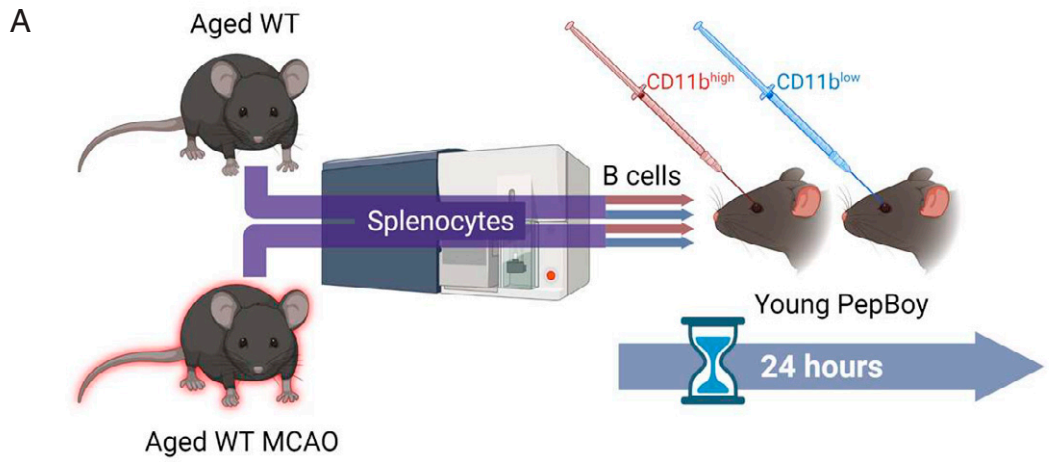

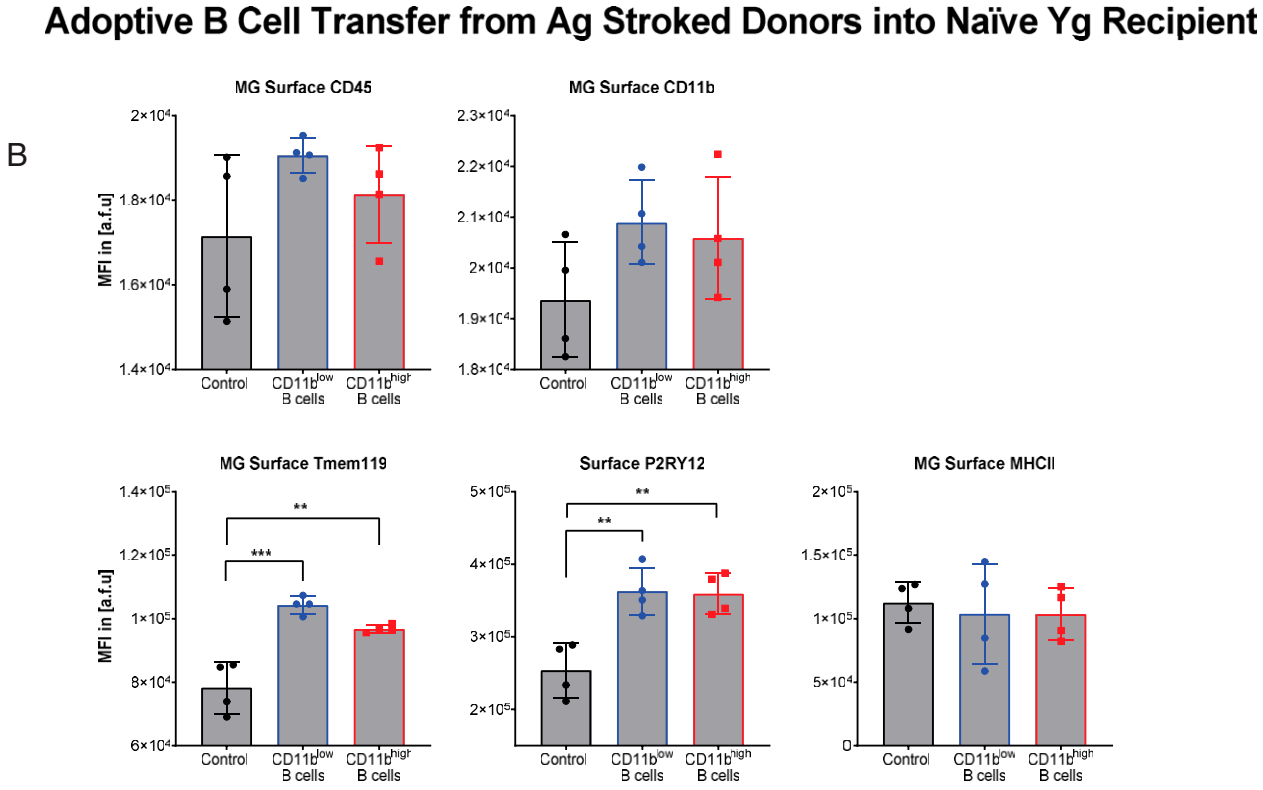

FIGURE 4. Differential MG surface phenotype after adoptive transfer of CD11b^{high} or CD11b^{low} B cells into young naive host. (**A**) Schematic showing splenocytes from naive and stroke aged (Ag) male C57BL/6 mice that underwent cell sorting to isolate CD11b^{high} and CD11b^{low} B cells. Cells were then adoptively transferred to young (Yg) PepBoy recipient mice via retroorbital injection to contribute to modulation of MG phenotype. (**B**) Surface profile of MG from Yg recipient mice after adoptive transfer from Ag stroke donors. CD45 and CD11b MFI had no significant difference in MG between vehicle control and CD11b^{high} or CD11b^{low} B cell recipients. Tmem119 MFI increased in MG in CD11b^{high} and CD11b^{low} B cell recipients compared with vehicle controls (CD11b^{high}, $p = 0.0014$; CD11b^{low}, $p = 0.0001$). P2RY12 increased in MG in CD11b^{high} and CD11b^{low} B cell recipients compared with vehicle controls (CD11b^{high}, $p = 0.0040$; CD11b^{low}, $p = 0.0032$). MHC-II MFI had no significant difference in MG between CD11b^{high} and CD11b^{low} B cell recipients and vehicle control. Experiments were performed once. Unpaired one-way ANOVA with Tukey's multiple comparisons test; mean ± SEM. $^{**}p < 0.01$, $^{***}p < 0.001$. WT, wild type.

increased on sorted B cells after a 48-h LPS stimulation when compared with B cells not treated with LPS isolated from the same animal (Supplemental Fig. 1B). We also examined T-bet expression levels of CD45$^+$CD19$^+$CD11b^{high} B cells and found that their relative frequency of T-bet$^+$ cells are significantly higher than that of their CD45$^+$CD19$^+$CD11b^{low} B cell counterparts (Supplemental Fig. 1C), which is consistent with their previously proposed age-associated B cell (ABC) phenotype (41).

We detected differences in phagocytic activity and cytokine production of CD11b^{high} B cells when compared with CD11b^{low} B cells. A phagocytosis assay was performed using 0.5 μm fluorescent beads incubated for 30 min with sorted CD45$^+$CD19$^+$CD11b^{high} and CD11b^{low}

B subsets from naive aged spleens and then analyzed by flow cytometry. Representative images of fluorescent beads with CD11b^{low} (left) compared with CD11b^{high} (right) B cells stained with DAPI were generated to visualize the uptake of beads by the B cells (Fig. 1E). Flow cytometric analysis of B cell phagocytic activity revealed a significant increase in the uptake of fluorescent beads in CD11b^{high} B cells compared with CD11b^{low} B cells (Fig. 1G). Previously described activated B cells in mice showed increased TNF-α production (51). Next, to determine if CD11b^{high} B cells produce cytokines capable of mediating proinflammatory activity in MG, TNF-α production was quantified in CD11b^{high} and CD11b^{low} B cells sorted as CD45$^+$CD19$^+$CD11b^{high} cells, sorted CD45$^+$CD19$^+$CD11b^{low} cells, sorted CD45$^+$CD19$^+$ cells, and unsorted splenocytes isolated from naive aged animals. This analysis revealed that CD11b^{high} B cells have a higher capacity for TNF-α production than CD11b^{low} B cells (Fig. 1F). Importantly, CD11b^{high} B cells did not depend on the presence of other immune cells for this effect (Fig. 1F). These findings indicate the activated state of these CD11b^{high} B cells in both Ag uptake and cytokine production.

CD11b^{high} B cells are increased in both young and aged brains as early as post–MCAO day 7

To test whether CD11b^{high} B cells increase in the brain after stroke, both young and aged mice underwent 60-min MCAO (Fig. 2A). At post-MCAO day 7, brain CD11b^{high} and CD11b^{low} B cells were compared in contralateral and ipsilateral hemispheres in stroke and sham animals. After stroke, both young and aged samples show an increase the density of immune populations, notably in CD11b^{high} B cells (Fig. 2B, red island). The ipsilateral stroke hemisphere in aged animals demonstrated a significant increase in absolute CD11b^{high} B cell counts ($p = 0.0019$), with young cells trending upward in number ($p = 0.0573$). The ipsilateral stroke hemisphere in aged animals demonstrated that stroke resulted in a significant increase in the percentage of CD11b^{high} B cells within the total CD45$^+$/CD19$^+$ B cell population (aged $p < 0.0001$ and young $p = 0.0027$) (Fig. 2C). Absolute counts of B cell populations are provided in Table II, and a representative Kaplan-Meier curve of MCAO mortality in young and aged mice is included in Fig. 2D.

Differential MG surface phenotype after stroke and after incubation with sorted CD11b^{high} or CD11b^{low} B cells

Next, CD45, CD11b, MHC-II, P2RY12, and Tmem119 were analyzed to assess MG activation from ipsilateral hemispheres in young (Fig. 3A) and aged (Fig. 3B) mice compared with either contralateral hemisphere or sham brain samples. The gating strategy for MG is provided (Supplemental Fig. 1D). Consistent with previous studies (2, 3, 52, 53), MFIs of CD45 and MHC-II were significantly increased, whereas P2RY12 and Tmem119 were significantly decreased, in young post-stroke MG (Fig. 3A). The surface profile of MG from aged mice after MCAO also revealed a significant increase in CD45 in the ipsilateral hemisphere as well as similar trends in MHC-II, P2RY12, and Tmem119 expression after MCAO (Fig. 3B). These results confirmed activation of MG after stroke in our model, which was also associated with a significantly increased presence of CD11b^{high} B cells in the brain.

To understand the role of CD11b^{high} B cells in the context of neuroinflammation, we assessed the ex vivo ability of CD11b^{high} B cells to induce changes to MG surface phenotype. Aged MG-enriched CNS mononuclear cell suspensions were divided across three coincubation conditions with sorted CD11b^{high} B cells, sorted CD11b^{low} B cells, and a control group. Sorted cells were derived from the spleen of the same animal. We hypothesized that CD11b^{high} B cells are capable of inducing an activated state in MG. Coincubation for 4 h with CD11b^{high} B cells compared with the control resulted in significantly increased Tmem119 expression levels, whereas CD11b^{low} B cells induced no changes (Fig. 3C). After a 24-h coincubation, there was a significant increase in CD45 expression in MG coincubated with sorted CD11b^{high} B cells compared with control, and the addition of CD11b^{low} B cells had no significant differences from the control group (Fig. 3D). Our data suggest that CD11b^{high} B cells can regulate MG activation. The increase of CD45 and decrease of Tmem119 indicate an activation state (3, 54–56).

To directly compare the capacity of CD11b^{high} and CD11b^{low} B cells to differentially influence MG surface phenotype responses, young and aged MG-enriched CNS mononuclear cells and sorted MG underwent 4-h coincubation using a broader panel of MG surface markers (CD45, CD11b, Tmem119, P2RY12, and MHC-II) (Supplemental Fig. 3A–3D). Young MG after 4-h coincubation with CD11b^{high} B cells compared with CD11b^{low} B cells resulted in relatively decreased CD45, CD11b, Tmem119, and P2RY12 expression levels (Supplemental Fig. 3A, top). Analysis of aged MG coincubated with B cells sorted from the same animals resulted in relatively decreased CD45 and Tmem119 expression (Supplemental Fig. 3A, bottom). Our data suggest that CD11b^{high} B cells can regulate MG activation unlike CD11b^{low} B cells. Reduction of CD45 and CD11b indicates a reduced activation state of MG, whereas decrease in Tmem119 and P2RY12 suggests an increased activation state of MG. Furthermore, aged MG appeared more resistant than young MG to changes in their surface phenotype.

We then evaluated surface expression of pure MG (sorted as live Tmem119$^+$) from both young and aged mice after a 4-h coincubation with sorted CD11b^{high} or CD11b^{low} B cells from aged splenocytes. Young MG after coincubation with CD11b^{high} B cells compared with CD11b^{low} B cells resulted in a relative decrease in CD45 and CD11b and no significant changes in Tmem119 and P2RY12 expression levels, and MHC-II had a relative decrease (Supplemental Fig. 3B, top). Aged MG showed no significant changes for CD45, CD11b, Tmem119, P2RY12, and MHC-II after coincubation with CD11b^{high} B cells compared with CD11b^{low} B cells (Supplemental Fig. 3B, bottom). These observations indicate that CD11b^{high} B cells can, independently of other immune cells, influence young MG but not aged MG. MG have been shown to alter their surface expression in ex vivo conditions (57). Therefore, our next step in understanding the

Table III. Absolute counts of total live and donor cells (CD45.2) in recipient mouse (CD45.1) 24 h after adoptive transfer by retroorbital injection

Sample	Detectable CD45.2 Cells	Number of Live Cells
01-Spleen-C1.fcs	78	275,637
01-Spleen-C2.fcs	31	285,155
01-Spleen-C3.fcs	60	278,033
01-Spleen-C4.fcs	65	270,406
01-Blood-E1.fcs	661	23,962
01-Blood-E2.fcs	208	11,333
01-Blood-E3.fcs	105	4946
01-Blood-E4.fcs	152	17,447
01-Skull-G1.fcs	347	27,276
01-Skull-G2.fcs	288	48,142
01-Skull-G3.fcs	318	62,906
01-Skull-G4.fcs	628	89,692
01-Brain-A1.fcs	234	10,208
01-Brain-A2.fcs	105	19,886
01-Brain-A3.fcs	178	15,527
01-Brain-A4.fcs	252	10,378
Tissue totals	**Transferred immune cells**	**Number of live cells**
Mouse 1	1320	337,083
Mouse 2	632	364,516
Mouse 3	661	361,412
Mouse 4	1097	387,923

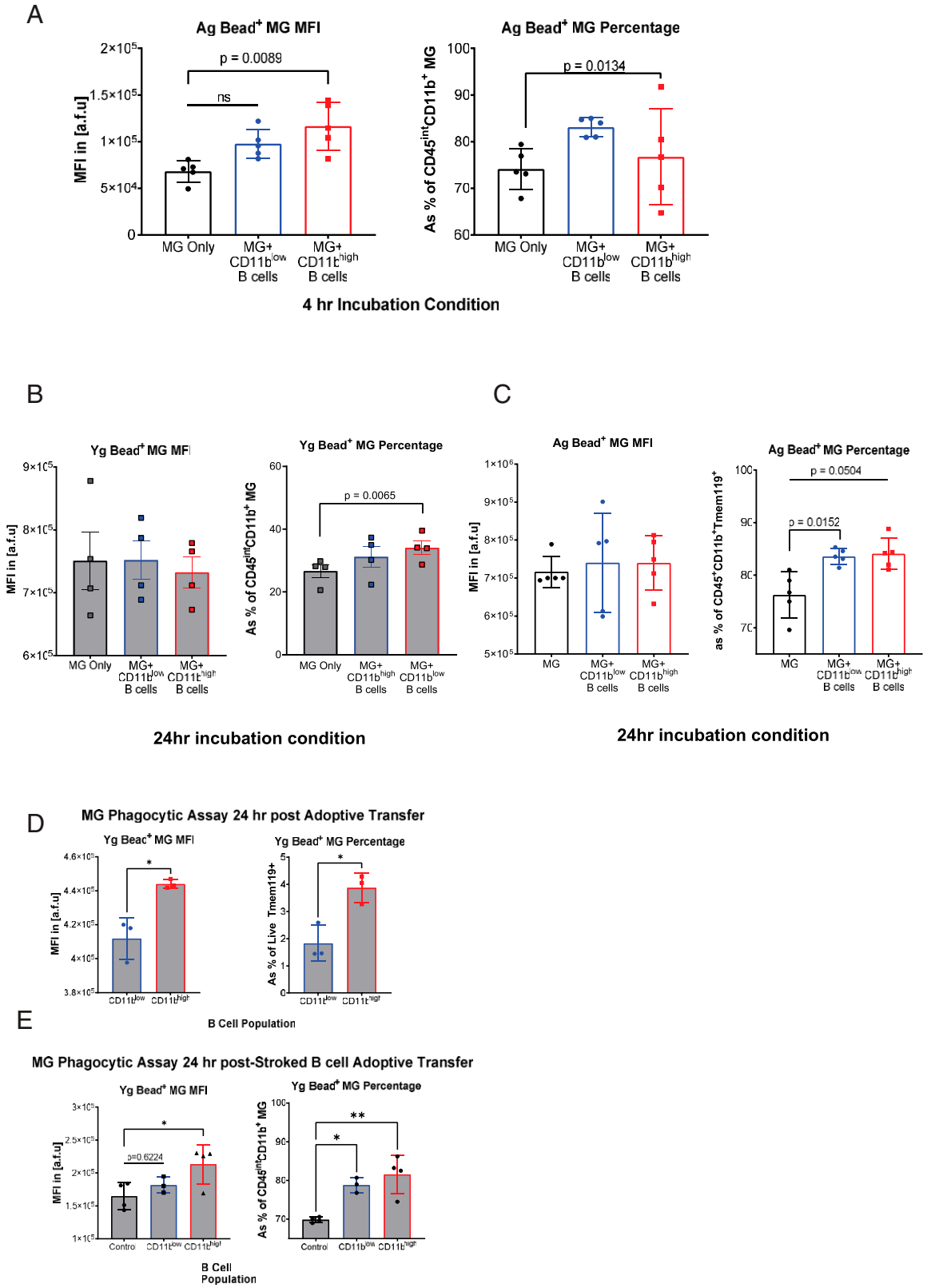

FIGURE 5. CD11b^{high} B cells increase MG phagocytosis. (**A**) Phagocytotic activity of 0.5 μm fluorescent beads by aged (Ag) MG after 4-h ex vivo coincubation ($n = 5$). Left, Measured bead MFI, with a significant increase ($p = 0.0089$), in MG incubated with CD11b^{high} B cells compared with MG alone. Right, Increased relative frequency of phagocytotic activity in MG incubated with CD11b^{low} B cells and compared with MG alone ($p = 0.0134$). (**B**) Relative frequency of phagocytotic activity in Ag (left) and young (Yg; right) MG after 24-h coincubation with no significant differences in *(Figure legend continues)*

effects of CD11b^{high} B cells on MG was to use an in vivo model of adoptive transfer.

Differential MG surface phenotype after adoptive transfer of CD11b^{high} or CD11b^{low} B cells into young naive host

Adoptive transfer can determine if increasing the number of CD11b^{high} B cells alters MG activation. We used PepBoy mice with a distinguishable CD45 haplotype (i.e., CD45.1) to carry out our adoptive B cell transfer experiments. First, spleen, blood, brain, and skull bone marrow underwent analysis to detect the presence of CD45.2^{+} cells in recipient mice 24 h after retroorbital injection. This validated that the cells from the donor mice were successfully transferred to the recipient in all tissues, and it indicated that CD11b^{high} B cells distribute throughout the host in the absence of injury (Table III). Next, sorted CD11b^{high} and CD11b^{low} B cells from the spleens of aged wild-type mice were transferred into young PepBoy mice (Fig. 4A). The brains of the recipient underwent analysis 24 h after injection. CD11b increased in MG in CD11b^{high} B cell recipients compared with CD11b^{low} B cell recipients (Supplemental Fig. 3D). CD11b increased in MG in CD11b^{high} B cell recipients compared with CD11b^{low} B cell recipients. CD45, CD11b, and MHC-II MFI had no significant difference in MG between vehicle control and CD11b^{high} or CD11b^{low} B cell recipients. Tmem119 and P2RY12 MFIs increased in MG in CD11b^{high} and CD11b^{low} B cell recipients compared with vehicle control (Fig. 4B). Our data suggest that although there were responses in MG due to the presence of additional B cells, there was no clear pattern of MG activation based on surface phenotyping alone. Next, we investigated the phagocytotic activity in MG as a response to ex vivo and in vivo stimulation with CD11b^{high} or CD11b^{low} B cells.

CD11b^{high} B cells increase MG phagocytosis

TNF-α has been shown to regulate MG phagocytosis (22, 24, 25, 58); thus, we tested whether CD11b^{high} B cells increase MG phagocytosis, given their higher capacity for TNF-α production (Fig. 1F). Phagocytotic activity of MG-enriched CNS mononuclear cells after 4 h (Fig. 5A) and 24 h (Fig. 5B, 5C) of coincubation with CD11b^{high} and CD11b^{low} B cell subsets was assessed. MG showed significantly increased phagocytosis after a 4-h ex vivo coincubation with CD11b^{high} B cells compared with controls, whereas CD11b^{low} B cells had no significant effect on the MFI of bead^{+} MG (Fig. 5A–5C). However, MG incubated with CD11b^{low} B cells had a greater percentage of bead^{+} MG (Fig. 5A–5C). Taken together, MG incubated with CD11b^{high} had higher phagocytosis capacity, even though the overall number of phagocytosing MG were similar in both MG incubated with CD11b^{low} and MG incubated with CD11b^{high} (Fig. 5A). Young and aged MG significantly increased their phagocytic activity after 24-h coincubation with CD11b^{high} B cells measured by relative frequency of bead positive MG (Fig. 5B, 5C).

Finally, phagocytosis assays of MG after adoptive B cell transfer from aged (Fig. 5D) and aged stroke (Fig. 5E) donors demonstrated that phagocytosis capacity of MG is significantly increased in MG from mice that received CD11b^{high} B cells compared with MG from mice that received CD11b^{low} B cells and vehicle control groups. Both ex vivo and in vivo data in our study consistently show that CD11b^{high} B cells can independently increase MG phagocytosis.

Discussion

The CNS has long been considered "immune privileged," a dogma that arose from studies by Medawar (59) and others, in which transplanting heterologous tissue into the CNS parenchyma failed to induce an effective immune response (60, 61). However, accumulating evidence of neuroimmune communication in the CNS in both homeostatic and pathological conditions has shifted this paradigm (62). The CNS contains MG that play a central role in both the acute and chronic phases of neuroinflammation. In addition, innate and adaptive immune cells in the CNS meninges take an active part in brain immune surveillance (63, 64). Pioneering work by Kipnis et al. (10, 12, 65) and others revealed an extensive network of meningeal lymphatics and their role in the neuroimmune interface, shedding light on the importance of central and peripheral immune interactions.

ABCs are a group of functionally distinct B cells that significantly increase in aged mice and in autoimmune diseases in humans (51). The surface phenotyping of these cells vary, and they contribute up to 30% of the mature B cell pool of aged mice (38–40, 51, 66). Here, we demonstrate that the CD11b^{high} subset of B cells have a distinct surface phenotype in the CNS and periphery, and we demonstrate increased TNF-α production and increased phagocytosis in ex vivo assays. The ABC phenotype has been associated with increased expression of T-bet (41, 67), a transcription factor essential for autoantibody production (68, 69). A significant increase in T-bet levels in the CD11b^{high} B cells was also seen in this study (Supplemental Fig. 1C), supporting that these CD11b^{high} B cells could be a subset of ABCs. We then determined that CD11b^{high} B cells have a distinct surface phenotype and are highly activated and heterogeneous, as demonstrated by higher expression of CD138 (expressed by plasma cells [70]), CD80 and CD27 (expressed by memory B cells [71, 72]), CD73 (expressed by class-switched B cells [73]), and CD268 (also known as BAFFR, expressed by B cells implicated in autoreactivity [31, 74]). This conclusion is further supported by the significant decrease in IgD with no significant change in IgM (Fig. 1D), a finding that is consistent with previous phenotyping of ABCs (35, 66). These findings combined, along with accumulation of CD11b^{high} B cells in the brain with aging and after neurologic injury, suggest that these cells could be considered as a subset of ABCs.

The amount of CD11b^{high} B cells increase significantly by post–MCAO day 7 in both young and aged brain, and this increase is associated with expected activation of MG after stroke when assessed by higher expression of CD45 and MHC-II but lower expression of Tmem119 and P2RY12 (3, 75). The function of Tmem119 is not yet understood; however, its decreased expression has been associated with activation of MG (56, 76–78). The increased expression of CD45 and MHC-II is characteristic of

bead MFI and a significant increased relative frequency of phagocytotic activity in MG incubated with CD11b^{high} B cells compared with MG alone ($p = 0.0065$; $n = 4$). (**C**) Ag MG had no significant differences in bead MFI and an increased relative frequency of phagocytotic activity in MG incubated with CD11b^{low} compared with MG alone ($p = 0.0504$). Paired one-way ANOVA with Dunnett's multiple comparisons test. (**D**) Phagocytotic activity of Yg MG after adoptively transferred Ag CD11b^{high} and CD11b^{low} B cells 24 h after transfer of B cell populations ($n = 3$). Left, Measured bead MFI, with a significant increase in MG in mice that received CD11b^{high} B cells compared and CD11b^{low} B cells ($p = 0.0116$). Right, Increased relative frequency of phagocytotic activity in MG incubated with CD11b^{high} and CD11b^{low} B cells ($p = 0.0140$). Unpaired t test. (**E**) Phagocytotic activity of Yg MG after adoptively transferred stroke Ag CD11b^{high} and CD11b^{low} B cells 24 h after transfer of B cell populations ($n = 3$ or 4). Left, Measured bead MFI with a significant increase in MG incubated with CD11b^{high} B cells compared with MG alone ($p = 0.0417$). Right, Increased relative frequency of phagocytotic activity in MG incubated with CD11b^{high} and CD11b^{low} B cells compared with MG alone ($p = 0.0023$ and 0.0154, respectively). (A) and (C) were independently reproduced in two experiments. (B), (D), and (E) experiments were performed once. One-way ANOVA post hoc Tukey's multiple comparison; mean ± SEM. *$p < 0.05$, **$p < 0.01$.

increased MG activation and phagocytosis (79, 80). Next, we sought to induce a strokelike MG activation state by coincubating sorted MG from young and aged brains with either CD11b^{high} or CD11b^{low} sorted B cells. We found that the CD11b^{high} B cells can distinctly modify surface phenotype and increased MG phagocytosis when compared with their CD11b^{low} counterparts ex vivo. Furthermore, 24 h after adoptively transferring CD11b^{high} B cells from both aged naive and aged stroke wild-type mice into young PepBoy mice, we observed a significant increase in phagocytosis in MG compared with CD11b^{low} transferred B cells. Given the increasing availability of U.S. Food and Drug Administration–approved B cell therapies for a variety of inflammatory conditions, better insight into the interaction between B cells and innate CNS immune cells is of high clinical relevance (81).

The infiltration of peripheral lymphocytes after stroke is a key feature of the progression of neuroinflammation, and B cell–derived cytokine production can influence outcomes after stroke (40, 82). Studies have shown that B cells contribute to post-stroke cognitive impairment (40, 82–84). Here, we demonstrated that CD11b^{high} B cells produce significantly higher amounts of TNF-α than CD11b^{low} B cells, and this increased production of TNF-α is correlated with ex vivo increased MG phagocytic activity, which is consistent with prior reports (22, 24, 25, 58, 85). By affecting MG activation and phagocytosis and possessing the chronic memory function, CD11b^{high} B cells have the ability to regulate long-term neurologic outcomes in aging and after cerebrovascular injury, as recently shown by a robust presence of ABCs in the meningeal layers (46). Therefore, we speculate that the increased activation of MG and their increased phagocytosis are a result, at least in part, of the presence of CD11b^{high} B cells and their high capacity to produce TNF-α. Future mechanistic studies using TNF receptor knockouts in MG can shed more light on the regulatory influence of TNF-α produced by CD11b^{high} B cells on MG-mediated neuroinflammation.

Previous studies have shown that flow cytometric analysis excludes CD11b^{high} B cells (42–45) or "infiltrating monocytes" that include CD11b^{high} B cells (86). As we demonstrate here, this gating strategy would only exclude a negligible fraction of the B cell population in young mice (Fig. 1A) and thus would be appropriate when using young uninjured animal models. However, in studies investigating B cells in brain injury or aging models, the exclusion of CD11b^{high} B cells will result in the exclusion of a significant subpopulation of B cells (Fig. 1A). Not only is this a large sum of cells to exclude but also, as we demonstrated here, CD11b^{high} B cells have increased cytokine production and phagocytic activity, and their exclusion may lead to skewed results in the assessment of B cell function in neuroinflammation. Therefore, careful validations should be performed when using flow cytometric identification of B cells in the context of neuroinflammation.

As both APCs and adaptive immune cells with memory function, B cells are uniquely positioned to regulate both acute and chronic phases of the post-stroke immune response, and their influence is subset specific. Future studies are warranted to better understand the function of CD11b^{high} B cells in neuroinflammation.

Acknowledgments

The figures were created in BioRender and published under agreement nos. KQ23P0DMSF and NE23P0D37X.

Disclosures

The authors have no financial conflicts of interest.

References

1. Roy-O'Reilly, M., and L. D. McCullough. 2018. Age and sex are critical factors in ischemic stroke pathology. *Endocrinology* 159: 3120–3131.
2. Ritzel, R. M., Y.-J. Lai, J. D. Crapser, A. R. Patel, A. Schrecengost, J. M. Grenier, N. S. Mancini, A. Patrizz, E. R. Jellison, D. Morales-Scheihing, et al. 2018. Aging alters the immunological response to ischemic stroke. *Acta Neuropathol.* 136: 89–110.
3. Honarpisheh, P., J. Lee, A. Banerjee, M. P. Blasco-Conesa, P. Honarpisheh, J. d'Aigle, A. A. Mamun, R. M. Ritzel, A. Chauhan, B. P. Ganesh, and L. D. McCullough. 2020. Potential caveats of putative microglia-specific markers for assessment of age-related cerebrovascular neuroinflammation. *J. Neuroinflammation* 17: 366.
4. Ritzel, R. M., J. He, Y. Li, T. Cao, N. Khan, B. Shim, B. Sabirzhanov, T. Aubrecht, B. A. Stoica, A. I. Faden, et al. 2021. Proton extrusion during oxidative burst in microglia exacerbates pathological acidosis following traumatic brain injury. *Glia* 69: 746–764.
5. Chauhan, A., A. Al Mamun, G. Spiegel, N. Harris, L. Zhu, and L. D. McCullough. 2018. Splenectomy protects aged mice from injury after experimental stroke. *Neurobiol. Aging* 61: 102–111.
6. Manwani, B., F. Liu, Y. Xu, R. Persky, J. Li, and L. D. McCullough. 2011. Functional recovery in aging mice after experimental stroke. *Brain Behav. Immun.* 25: 1689–1700.
7. Sieber, M. W., R. A. Claus, O. W. Witte, and C. Frahm. 2011. Attenuated inflammatory response in aged mice brains following stroke. *PLoS One* 6: e26288.
8. Manwani, B., F. Liu, V. Scranton, M. D. Hammond, L. H. Sansing, and L. D. McCullough. 2013. Differential effects of aging and sex on stroke induced inflammation across the lifespan. *Exp. Neurol.* 249: 120–131.
9. Shi, L., Z. Sun, W. Su, F. Xu, D. Xie, Q. Zhang, X. Dai, K. Iyer, T. K. Hitchens, L. M. Foley, et al. 2021. Treg cell-derived osteopontin promotes microglia-mediated white matter repair after ischemic stroke. *Immunity* 54: 1527–1542.e8.
10. Radjavi, A., I. Smirnov, N. Derecki, and J. Kipnis. 2014. Dynamics of the meningeal CD4^{+} T-cell repertoire are defined by the cervical lymph nodes and facilitate cognitive task performance in mice. *Mol. Psychiatry* 19: 531–532.
11. Mastorakos, P., and D. McGavern. 2019. The anatomy and immunology of vasculature in the central nervous system. *Sci. Immunol.* 4: eaav0492.
12. Rustenhoven, J., A. Drieu, T. Mamuladze, K. A. de Lima, T. Dykstra, M. Wall, Z. Papadopoulos, M. Kanamori, A. F. Salvador, W. Baker, et al. 2021. Functional characterization of the dural sinuses as a neuroimmune interface. *Cell* 184: 1000–1016.e27.
13. Candlish, M., and J. K. Hefendehl. 2021. Microglia phenotypes converge in aging and neurodegenerative disease. *Front. Neurol.* 12: 660720.
14. Greenwood, E. K., and D. R. Brown. 2021. Senescent microglia: the key to the ageing brain? *Int. J. Mol. Sci.* 22: 4402.
15. Martinez, F., J. Novarino, J. E. Mejía, N. Fazilleau, and M. Aloulou. 2021. Ageing of T-dependent B cell responses. *Immunol. Lett.* 233: 97–103.
16. Xie, X., J. Shrimpton, G. M. Doody, P. G. Conaghan, and F. Ponchel. 2021. B-cell capacity for differentiation changes with age. *Aging Cell* 20: e13341.
17. Norden, D. M., and J. P. Godbout. 2013. Review: microglia of the aged brain: primed to be activated and resistant to regulation. *Neuropathol. Appl. Neurobiol.* 39: 19–34.
18. Gosselin, D., D. Skola, N. G. Coufal, I. R. Holtman, J. C. M. Schlachetzki, E. Sajti, B. N. Jaeger, C. O'Connor, C. Fitzpatrick, M. P. Pasillas, et al. 2017. An environment-dependent transcriptional network specifies human microglia identity. *Science* 356: 1248–1259.
19. Li, K., W. Yu, R. Cao, Z. Zhu, and G. Zhao. 2017. Microglia-mediated BAFF-BAFFR ligation promotes neuronal survival in brain ischemia injury. *Neuroscience* 363: 87–96.
20. Honarpisheh, P., F. W. Blixt, M. P. Blasco Conesa, W. Won, J. d'Aigle, Y. Munshi, J. Hudobenko, J. W. Furr, A. Mobley, J. Lee, et al. 2020. Peripherally-sourced myeloid antigen presenting cells increase with advanced aging. *Brain Behav. Immun.* 90: 235–247.
21. Oishi, Y., and I. Manabe. 2016. Macrophages in age-related chronic inflammatory diseases. *NPJ Aging Mech. Dis.* 2: 16018.
22. Harms, A. S., J.-K. Lee, T. A. Nguyen, J. Chang, K. M. Ruhn, I. Treviño, and M. G. Tansey. 2012. Regulation of microglia effector functions by tumor necrosis factor signaling. *Glia* 60: 189–202.
23. McCoy, M. K., and M. G. Tansey. 2008. TNF signaling inhibition in the CNS: implications for normal brain function and neurodegenerative disease. *J. Neuroinflammation* 5: 45.
24. Lively, S., and L. C. Schlichter. 2018. Microglia responses to pro-inflammatory stimuli (LPS, IFNγ+TNFα) and reprogramming by resolving cytokines (IL-4, IL-10). *Front. Cell. Neurosci.* 12: 215.
25. Neniskyte, U., A. Vilalta, and G. C. Brown. 2014. Tumour necrosis factor alpha-induced neuronal loss is mediated by microglial phagocytosis. *FEBS Lett.* 588: 2952–2956.
26. Frasca, D., A. Diaz, M. Romero, A. M. Landin, and B. B. Blomberg. 2014. High TNF-α levels in resting B cells negatively correlate with their response. *Exp. Gerontol.* 54: 116–122.
27. Ren, X., K. Akiyoshi, S. Dziennis, A. A. Vandenbark, P. S. Herson, P. D. Hurn, and H. Offner. 2011. Regulatory B cells limit CNS inflammation and neurologic deficits in murine experimental stroke. *J. Neurosci.* 31: 8556–8563.
28. Chen, Y., S. Bodhankar, S. J. Murphy, A. A. Vandenbark, N. J. Alkayed, and H. Offner. 2012. Intrastriatal B-cell administration limits infarct size after stroke in B-cell deficient mice. *Metab. Brain Dis.* 27: 487–493.
29. Zhou, T., Y. Zheng, L. Sun, S. R. Badea, Y. Jin, Y. Liu, A. J. Rolfe, H. Sun, X. Wang, Z. Cheng, et al. 2019. Microvascular endothelial cells engulf myelin debris and promote macrophage recruitment and fibrosis after neural injury. *Nat. Neurosci.* 22: 421–435.

30. Planas, A. M., M. Gómez-Choco, X. Urra, R. Gorina, M. Caballero, and Á. Chamorro. 2012. Brain-derived antigens in lymphoid tissue of patients with acute stroke. *J. Immunol.* 188: 2156–2163.
31. Liu, X., X. Jiang, R. Liu, L. Wang, T. Qian, Y. Zheng, Y. Deng, E. Huang, F. Xu, J.-Y. Wang, and Y. Chu. 2015. B cells expressing CD11b effectively inhibit $CD4^+$ T-cell responses and ameliorate experimental autoimmune hepatitis in mice. *Hepatology* 62: 1563–1575.
32. Schittenhelm, L., C. M. Hilkens, and V. L. Morrison. 2017. β_2 Integrins as regulators of dendritic cell, monocyte, and macrophage function. *Front. Immunol.* 8: 1866.
33. Jenks, S. A., K. S. Cashman, E. Zumaquero, U. M. Marigorta, A. V. Patel, X. Wang, D. Tomar, M. C. Woodruff, Z. Simon, R. Bugrovsky, et al. 2018. Distinct effector B cells induced by unregulated Toll-like receptor 7 contribute to pathogenic responses in systemic lupus erythematosus. [Published erratum appears in 2020 *Immunity* 52: 203.] *Immunity* 49: 725–739.e6.
34. Wang, S., J. Wang, V. Kumar, J. L. Karnell, B. Naiman, P. S. Gross, S. Rahman, K. Zerrouki, R. Hanna, C. Morehouse, et al.; Autoimmunity Molecular Medicine Team. 2018. IL-21 drives expansion and plasma cell differentiation of autoreactive $CD11c^{hi}T\text{-}bet^+$ B cells in SLE. *Nat. Commun.* 9: 1758.
35. Hao, Y., P. O'Neill, M. S. Naradikian, J. L. Scholz, and M. P. Cancro. 2011. A B-cell subset uniquely responsive to innate stimuli accumulates in aged mice. *Blood* 118: 1294–1304.
36. Yousefzadeh, M. J., R. R. Flores, Y. Zhu, Z. C. Schmiechen, R. W. Brooks, C. E. Trussoni, Y. Cui, L. Angelini, K.-A. Lee, S. J. McGowan, et al. 2021. An aged immune system drives senescence and ageing of solid organs. *Nature* 594: 100–105.
37. Lindestam Arlehamn, C. S., J. Pham, R. N. Alcalay, A. Frazier, E. Shorr, C. Carpenter, J. Sidney, R. Dhanwani, J. Agin-Liebes, F. Garretti, et al. 2019. Widespread tau-specific CD4 T cell reactivity in the general population. *J. Immunol.* 203: 84–92.
38. Du, S. W., T. Arkatkar, F. Al Qureshah, H. M. Jacobs, C. D. Thouvenel, K. Chiang, A. D. Largent, Q. Z. Li, B. Hou, D. J. Rawlings, and S. W. Jackson. 2019. Functional characterization of $CD11c^+$ age-associated B cells as memory B cells. *J. Immunol.* 203: 2817–2826.
39. Blanco, E., M. Pérez-Andrés, S. Arriba-Méndez, T. Contreras-Sanfeliciano, I. Criado, O. Pelak, A. Serra-Caetano, A. Romero, N. Puig, A. Remesal, et al.; EuroFlow PID group. 2018. Age-associated distribution of normal B-cell and plasma cell subsets in peripheral blood. *J. Allergy Clin. Immunol.* 141: 2208–2219.e16.
40. Doyle, K. P., and M. S. Buckwalter. 2020. Immunological mechanisms in post-stroke dementia. *Curr. Opin. Neurol.* 33: 30–36.
41. Rubtsova, K., A. V. Rubtsov, M. P. Cancro, and P. Marrack. 2015. Age-associated B cells: a T-bet-dependent effector with roles in protective and pathogenic immunity. *J. Immunol.* 195: 1933–1937.
42. Weitbrecht, L., D. Berchtold, T. Zhang, S. Jagdmann, C. Dames, K. Winek, C. Meisel, and A. Meisel. 2021. $CD4^+$ T cells promote delayed B cell responses in the ischemic brain after experimental stroke. *Brain Behav. Immun.* 91: 601–614.
43. Harp, C. R. P., A. S. Archambault, M. Cheung, J. W. Williams, R. S. Czepielewski, P. C. Duncker, A. J. Kilgore, A. T. Miller, B. M. Segal, A. H. J. Kim, et al. 2019. Neutrophils promote VLA-4-dependent B cell antigen presentation and accumulation within the meninges during neuroinflammation. *Proc. Natl. Acad. Sci. USA* 116: 24221–24230.
44. Bodhankar, S., Y. Chen, A. A. Vandenbark, S. J. Murphy, and H. Offner. 2014. Treatment of experimental stroke with IL-10-producing B-cells reduces infarct size and peripheral and CNS inflammation in wild-type B-cell-sufficient mice. *Metab. Brain. Dis.* 29: 59–73.
45. Harp, C. R. P., A. S. Archambault, J. Sim, S. T. Ferris, R. J. Mikesell, P. A. Koni, M. Shimoda, C. Linington, J. H. Russell, and G. F. Wu. 2015. B cell antigen presentation is sufficient to drive neuroinflammation in an animal model of multiple sclerosis. *J. Immunol.* 194: 5077–5084.
46. Schafflick, D., J. Wolbert, M. Heming, C. Thomas, M. Hartlehnert, A.-L. Börsch, A. Ricci, S. Martín-Salamanca, X. Li, I.-N. Lu, et al. 2021. Single-cell profiling of CNS border compartment leukocytes reveals that B cells and their progenitors reside in non-diseased meninges. *Nat. Neurosci.* 24: 1225–1234.
47. Chauhan, A., H. Moser, and L. D. McCullough. 2017. Sex differences in ischaemic stroke: potential cellular mechanisms. *Clin. Sci. (Lond.)* 131: 533–552.
48. Verma, R., R. M. Ritzel, N. M. Harris, J. Lee, T. Kim, G. Pandi, R. Vemuganti, and L. D. McCullough. 2018. Inhibition of miR-141-3p ameliorates the negative effects of poststroke social isolation in aged mice. *Stroke* 49: 1701–1707.
49. Lee, J., J. d'Aigle, L. Atadja, V. Quaicoe, P. Honarpisheh, B. P. Ganesh, A. Hassan, J. Graf, J. Petrosino, N. Putluri, et al. 2020. Gut microbiota-derived short-chain fatty acids promote poststroke recovery in aged mice. *Circ. Res.* 127: 453–465.
50. Rangaraju, S., S. A. Raza, N. X. Li, R. Betarbet, E. B. Dammer, D. Duong, J. J. Lah, N. T. Seyfried, and A. I. Levey. 2018. Differential phagocytic properties of $CD45^{low}$ microglia and $CD45^{high}$ brain mononuclear phagocytes-activation and age-related effects. *Front. Immunol.* 9: 405.
51. Ma, S., C. Wang, X. Mao, and Y. Hao. 2019. B cell dysfunction associated with aging and autoimmune diseases. *Front. Immunol.* 10: 318.
52. Kronenberg, G., R. Uhlemann, N. Richter, F. Klempin, S. Wegner, L. Staerck, S. Wolf, W. Uckert, H. Kettenmann, M. Endres, and K. Gertz. 2018. Distinguishing features of microglia- and monocyte-derived macrophages after stroke. *Acta Neuropathol.* 135: 551–568.
53. Rawlinson, C., S. Jenkins, L. Thei, M. L. Dallas, and R. Chen. 2020. Post-ischaemic immunological response in the brain: targeting microglia in ischaemic stroke therapy. *Brain Sci.* 10: 159.
54. Cao, Z., S. S. Harvey, T. Chiang, A. G. Foltz, A. G. Lee, M. Y. Cheng, and G. K. Steinberg. 2021. Unique subtype of microglia in degenerative thalamus after cortical stroke. *Stroke* 52: 687–698.
55. Rajan, W. D., B. Wojtas, B. Gielniewski, A. Gieryng, M. Zawadzka, and B. Kaminska. 2019. Dissecting functional phenotypes of microglia and macrophages in the rat brain after transient cerebral ischemia. *Glia* 67: 232–245.
56. Satoh, J., Y. Kino, N. Asahina, M. Takitani, J. Miyoshi, T. Ishida, and Y. Saito. 2016. TMEM119 marks a subset of microglia in the human brain. *Neuropathology* 36: 39–49.
57. Hasselmann, J., M. A. Coburn, W. England, D. X. Figueroa Velez, S. Kiani Shabestari, C. H. Tu, A. McQuade, M. Kolahdouzan, K. Echeverria, C. Claes, et al. 2019. Development of a chimeric model to study and manipulate human microglia in vivo. *Neuron* 103: 1016–1033.e10.
58. Sriram, K., J. M. Matheson, S. A. Benkovic, D. B. Miller, M. I. Luster, and J. P. O'Callaghan. 2006. Deficiency of TNF receptors suppresses microglial activation and alters the susceptibility of brain regions to MPTP-induced neurotoxicity: role of TNF-α. *FASEB J.* 20: 670–682.
59. Medawar, P. B. 1948. Immunity to homologous grafted skin; the fate of skin homografts transplanted to the brain, to subcutaneous tissue, and to the anterior chamber of the eye. *Br. J. Exp. Pathol.* 29: 58–69.
60. Widner, H., and P. Brundin. 1988. Immunological aspects of grafting in the mammalian central nervous system. A review and speculative synthesis. *Brain Res. Rev.* 13: 287–324.
61. Murphy, J. B., and E. Sturm. 1923. Conditions determining the transplantability of tissues in the brain. *J. Exp. Med.* 38: 183–197.
62. Louveau, A., T. H. Harris, and J. Kipnis. 2015. Revisiting the mechanisms of CNS immune privilege. *Trends Immunol.* 36: 569–577.
63. Mrdjen, D., A. Pavlovic, F. J. Hartmann, B. Schreiner, S. G. Utz, B. P. Leung, I. Lelios, F. L. Heppner, J. Kipnis, D. Merkler, et al. 2018. High-Dimensional single-cell mapping of central nervous system immune cells reveals distinct myeloid subsets in health, aging, and disease. [Published erratum appears in 2018 *Immunity* 48: 599.] *Immunity* 48: 380–395.e6.
64. Van Hove, H., L. Martens, I. Scheyltjens, K. De Vlaminck, A. R. Pombo Antunes, S. De Prijck, N. Vandamme, S. De Schepper, G. Van Isterdael, C. L. Scott, et al. 2019. A single-cell atlas of mouse brain macrophages reveals unique transcriptional identities shaped by ontogeny and tissue environment. *Nat. Neurosci.* 22: 1021–1035.
65. Da Mesquita, S., Z. Fu, and J. Kipnis. 2018. The meningeal lymphatic system: a new player in neurophysiology. *Neuron* 100: 375–388.
66. Rubtsov, A. V., K. Rubtsova, A. Fischer, R. T. Meehan, J. Z. Gillis, J. W. Kappler, and P. Marrack. 2011. Toll-like receptor 7 (TLR7)-driven accumulation of a novel $CD11c^+$ B-cell population is important for the development of autoimmunity. *Blood* 118: 1305–1315.
67. Myles, A., P. J. Gearhart, and M. P. Cancro. 2017. Signals that drive T-bet expression in B cells. *Cell. Immunol.* 321: 3–7.
68. Naradikian, M. S., A. Myles, D. P. Beiting, K. J. Roberts, L. Dawson, R. S. Herati, B. Bengsch, S. L. Linderman, E. Stelekati, R. Spolski, et al. 2016. Cutting edge: IL-4, IL-21, and IFN-γ interact to govern T-bet and CD11c expression in TLR-activated B cells. *J. Immunol.* 197: 1023–1028.
69. Peng, S. L., S. J. Szabo, and L. H. Glimcher. 2002. T-bet regulates IgG class switching and pathogenic autoantibody production. *Proc. Natl. Acad. Sci. USA* 99: 5545–5550.
70. Sanderson, R. D., P. Lalor, and M. Bernfield. 1989. B lymphocytes express and lose syndecan at specific stages of differentiation. *Cell Regul.* 1: 27–35.
71. Good-Jacobson, K. L., E. Song, S. Anderson, A. H. Sharpe, and M. J. Shlomchik. 2012. CD80 expression on B cells regulates murine T follicular helper development, germinal center B cell survival, and plasma cell generation. *J. Immunol.* 188: 4217–4225.
72. Wu, Y. C. B., D. Kipling, and D. K. Dunn-Walters. 2011. The relationship between CD27 negative and positive B cell populations in human peripheral blood. *Front. Immunol.* 2: 81.
73. Schneider, E., A. Rissiek, R. Winzer, B. Puig, B. Rissiek, F. Haag, H.-W. Mittrücker, T. Magnus, and E. Tolosa. 2019. Generation and function of non-cell-bound CD73 in inflammation. *Front. Immunol.* 10: 1729.
74. Qian, T., J. Hong, L. Wang, Z. Wang, Z. Lu, Y. Li, R. Liu, and Y. Chu. 2019. Regulation of CD11b by HIF-1α and the STAT3 signaling pathway contributes to the immunosuppressive function of B cells in inflammatory bowel disease. *Mol. Immunol.* 111: 162–171.
75. Ronaldson, P. T., and T. P. Davis. 2020. Regulation of blood-brain barrier integrity by microglia in health and disease: a therapeutic opportunity. *J. Cereb. Blood Flow Metab.* 40(1_suppl): S6–S24.
76. Bennett, M. L., F. C. Bennett, S. A. Liddelow, B. Ajami, J. L. Zamanian, N. B. Fernhoff, S. B. Mulinyawe, C. J. Bohlen, A. Adil, A. Tucker, et al. 2016. New tools for studying microglia in the mouse and human CNS. *Proc. Natl. Acad. Sci. USA* 113: E1738–E1746.
77. Zrzavy, T., S. Hametner, I. Wimmer, O. Butovsky, H. L. Weiner, and H. Lassmann. 2017. Loss of 'homeostatic' microglia and patterns of their activation in active multiple sclerosis. *Brain* 140: 1900–1913.
78. Bohnert, S., A. Seiffert, S. Trella, M. Bohnert, L. Distel, B. Ondruschka, and C. M. Monoranu. 2020. TMEM119 as a specific marker of microglia reaction in traumatic brain injury in postmortem examination. *Int. J. Legal Med.* 134: 2167–2176.
79. Chen, H. R., Y. Y. Sun, C. W. Chen, Y. M. Kuo, I. S. Kuan, Z. R. Tiger Li, J. C. Short-Miller, M. R. Smucker, and C. Y. Kuan. 2020. Fate mapping via CCR2-CreER mice reveals monocyte-to-microglia transition in development and neonatal stroke. *Sci. Adv.* 6: eabb2119.
80. Garner, K. M., R. Amin, R. W. Johnson, E. J. Scarlett, and M. D. Burton. 2018. Microglia priming by interleukin-6 signaling is enhanced in aged mice. *J. Neuroimmunol.* 324: 90–99.

81. Kamel, H., and C. Iadecola. 2012. Brain-immune interactions and ischemic stroke: clinical implications. *Arch. Neurol.* 69: 576–581.
82. Iadecola, C., M. S. Buckwalter, and J. Anrather. 2020. Immune responses to stroke: mechanisms, modulation, and therapeutic potential. *J. Clin. Invest.* 130: 2777–2788.
83. Doyle, K. P., L. N. Quach, M. Solé, R. C. Axtell, T. V. V. Nguyen, G. J. Soler-Llavina, S. Jurado, J. Han, L. Steinman, F. M. Longo, et al. 2015. B-lymphocyte-mediated delayed cognitive impairment following stroke. *J. Neurosci.* 35: 2133–2145.
84. Tsai, A. S., K. Berry, M. M. Beneyto, D. Gaudilliere, E. A. Ganio, A. Culos, M. S. Ghaemi, B. Choisy, K. Djebali, J. F. Einhaus, et al. 2019. A year-long immune profile of the systemic response in acute stroke survivors. *Brain* 142: 978–991.
85. Mir, M., L. Tolosa, V. J. Asensio, J. Lladó, and G. Olmos. 2008. Complementary roles of tumor necrosis factor alpha and interferon gamma in inducible microglial nitric oxide generation. *J. Neuroimmunol.* 204: 101–109.
86. Monson, N. L., S. B. Ortega, S. J. Ireland, A. J. Meeuwissen, D. Chen, E. J. Plautz, E. Shubel, X. Kong, M. K. Li, L. H. Freriks, and A. M. Stowe. 2014. Repetitive hypoxic preconditioning induces an immunosuppressed B cell phenotype during endogenous protection from stroke. *J. Neuroinflammation* 11: 22.